Endoscopic 3D-OCT reveals buried glands following radiofrequency ablation of Barrett's esophagus

Massachusetts Institute of Technology

Endoscopic 3D-OCT Reveals Buried Glands following Radiofrequency Ablation of Barrett's Esophagus

Chao Zhou[1*], Desmond C. Adler[1,2], Tsung-Han Tsai[1], Hsiang-Chieh Lee[1], Laren Becker[3,4], Joseph M. Schmitt[2], Qin Huang[3,4], James G. Fujimoto[1], Hiroshi Mashimo[3,4]

[1]Department of Electrical Engineering & Computer Science and Research Laboratory of Electronics, Massachusetts Institute of Technology, Cambridge, MA, USA
[2]LightLab Imaging Inc., Westford, MA, USA
[3]VA Healthcare System Boston, Boston, MA, USA
[4]Harvard Medical School, Boston, MA, USA

Abstract

Barrett's esophagus (BE) with high-grade dysplasia is generally treated by endoscopic mucosal resection or esophagectomy. Radiofrequency ablation (RFA) is a recent treatment that allows broad and superficial ablation for BE. Endoscopic three-dimensional optical coherence tomography (3D-OCT) is a volumetric imaging technique that is uniquely suited for follow-up surveillance of RFA treatment. 3D-OCT uses a thin fiberoptic imaging catheter placed down the working channel of a conventional endoscope. 3D-OCT enables *en face* and cross-sectional evaluation of the esophagus for detection of residual BE, neo-squamous mucosa, or buried BE glands. Patients who had undergone RFA treatment with the BARRX HALO90 system were recruited and imaged with endoscopic 3D-OCT before and after (3-25 months) RFA treatment. 3D-OCT findings were compared to pinch biopsy to confirm the presence or absence of squamous epithelium or buried BE glands following RFA. Gastric, BE, and squamous epithelium were readily distinguished from 3D-OCT over a large volumetric field of view (8mmx20mmx1.6 mm) with ~5µm axial resolution. In all patients, neo-squamous epithelium (NSE) was observed in regions previously treated with RFA. A small number of isolated glands were found buried beneath the regenerated NSE and lamina propria. NSE is a marker of successful ablative therapy, while buried glands may have malignant potential and are difficult to detect using conventional video endoscopy and random biopsy. Buried glands were not observed with pinch biopsy due to their extremely sparse distribution. These results indicate a potential benefit of endoscopic 3D-OCT for follow-up assessment of ablative treatments for BE.

Keywords: Optical coherence tomography; Barrett's esophagus; Radiofrequency ablation; Endoscope.

INTRODUCTION

Endoscopic ablative procedures such as photodynamic therapy, argon plasma coagulation, and radiofrequency ablation (RFA) are becoming increasingly common for treatment of Barrett's esophagus (BE). Residual BE regions that were not completely ablated and buried BE glands beneath regenerative neo-squamous epithelium (NSE) are found to varying degrees on follow-up, depending on the type of ablative therapy [1]. Detection of residual disease is critical to ensure that subsequent treatments are applied as necessary to completely remove the pathologic tissue. Conversely, detection of NSE is a hallmark of successful ablative therapy and could be used to confirm efficacious treatment. Buried BE glands are thought to represent lower malignant risk than untreated or residual BE, although there is still potential for buried BE glands to progress to dysplasia or adenocarcinoma [1, 2]. Detection of small areas of residual BE, buried BE glands, and NSE can be challenging using conventional video endoscopy and pinch biopsy [1], due to the diminutive size and sub-surface nature of these tissue types.

* chaozhou@mit.edu; Fax: 617-253-9611; 77 Massachusetts Ave, Room 36-357, Cambridge, MA, 02139.

Optical coherence tomography (OCT) is a cross-sectional and three-dimensional optical imaging technique analogous to ultrasound [3]. OCT provides micrometer-scale spatial resolutions with millimeter-scale tissue imaging depths by measuring the echo time delays of light back-reflected from the tissue. OCT can be performed with flexible fiber optic probes for endoscopic visualization of tissue architectural morphology [4]. More recently, endoscopic three-dimensional OCT (3D-OCT), also referred to as optical frequency domain imaging (OFDI), has become possible owing to dramatic increases in image acquisition speeds [5-7]. 3D-OCT is a powerful advance in imaging technology compared to the previous generation of two-dimensional (2D) OCT systems and allows comprehensive visualization of tissue microstructure in arbitrary *en face* and cross-sectional planes, providing a 3D endoscopic microscopy tool with an unmatched combination of high spatial resolution, large field of view, and rapid data acquisition [8-10].

2D-OCT has been extensively studied for applications in BE including the detection of specialized intestinal metaplasia, dysplasia, and adenocarcinoma [11-14]. 3D-OCT has recently been investigated in small pilot studies for esophageal imaging [8, 10] as well as for imaging a variety of pathologies in the human colon [9]. In this study, we report 3D-OCT endoscopic microscopy findings in patients with non-ablated BE glands and buried BE glands beneath NSE following RFA.

METHODS

After obtaining informed consent, we imaged 6 patients with endoscopic 3D-OCT before and after (3-25 months) RFA treatment for BE. Subjects followed a standard preparation procedure for upper endoscopy prior to the endoscopy appointment. 3D-OCT imaging was conducted using a spiral-scanning fiberoptic probe passed down the working channel of a standard esophagogastroduodenoscope (GIF Q180; Olympus, Tokyo, Japan), which enabled simultaneous video endoscopy examination. The endoscope was advanced to the region of interest and the 3D-OCT probe was subsequently positioned adjacent to the esophageal wall under endoscopic guidance. Endoscopic suction was applied to partially collapse the lumen around the probe, maximizing the amount of tissue within the imaging range of the 3D-OCT system. Biopsy samples were obtained from the imaged regions and prepared using a standard hematoxylin and eosin stain for comparison to the endoscopic microscopy data. RFA treatment was performed with the HALO90 system (BARRX Medical, Inc.). All patients tolerated the procedure well and there were no known complications associated with the study.

A detailed description of the 3D-OCT imaging system can be found in a recent publication from our group [9]. Briefly, 3D-OCT imaging was conducted using a catheter-based system that enables an unprecedented combination of field of view, resolution, and depth-sectioning capabilities. The system had a lateral resolution of 14 μm and axial resolution of 5μm. The outer diameter of the OCT probe is ~2.5 mm. 8 mm circumferential scans were acquired in a spiral pattern over a 20 mm pullback length with a depth penetration of ~1.6 mm in 20 seconds during a single acquisition, providing 3D endoscopic microscopy visualization over a large field of view. Volumetric data is acquired at 60,000 axial lines per second and 60 frames per second using a rotary fibre-optic endoscope probe. The volumetric data was therefore cylindrical in nature, but was converted to rectangular form using a "virtual incision" and unfolding image processing routine [6, 8, 9] to enable better visualization of *en face* tissue features and comparison to histology. 3D-OCT findings were compared to standard pinch biopsies to confirm the presence or absence of squamous epithelium, specialized intestinal metaplasia, or buried BE glands following RFA.

RESULTS

The first example is from a non-ablated BE patient, who was an 87 year old male with BE islands near the GE junction. The patient was first diagnosed with short-segment BE in 1991 and had been on a proton pump inhibitor (PPI) regimen for over 15 years. The patient had not previously received ablative treatments of any kind.
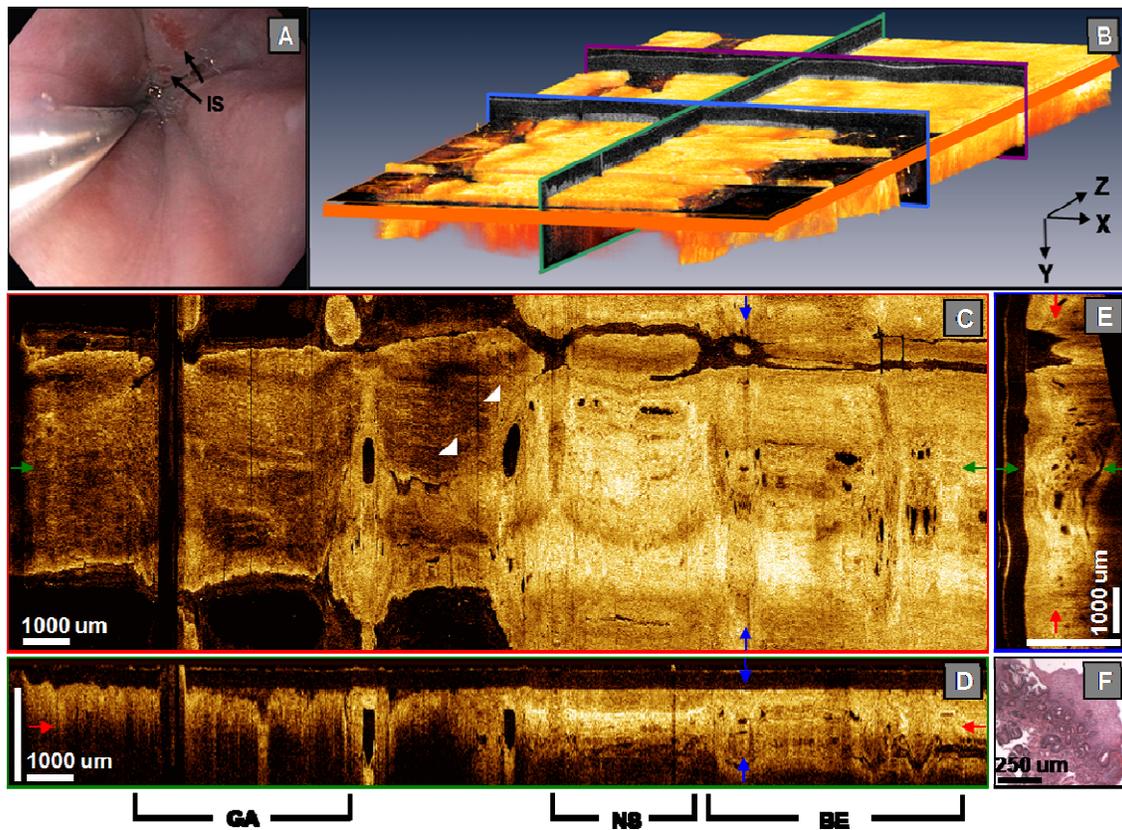
Figure 1. 3D-OCT images of BE glands near the GE junction (GEJ) in a non-ablated patient. A: Conventional white light endoscopy shows isolated BE islands (IS) at the GEJ. B: Volume rendering shows location of orthogonal cut planes. C: *En face* XZ image at 345 um tissue depth. The GEJ (arrows) can be clearly appreciated as the tissue architecture transits from gastric mucosa (left) to esophageal mucosa (right). Irregular glandular features are apparent. D: YZ Cross-section. Gastric (GA), normal squamous (NS), and BE regions can be distinguished. E: XY cross-section showing BE glands. F: H&E histology from the same area imaged with 3D-OCT.

Conventional endoscopic examination of the distal esophagus (Figure 1A) showed discrete regions of salmon-pink mucosa consistent with BE islands. Figure 1B shows 3D-OCT volumetric rendering data obtained from the esophagus, with the locations of orthogonal cut planes highlighted. 3D-OCT data spanning the gastro-esophageal junction (GEJ) are shown in Figure 1C-E. At a depth of 345 μm Figure 1C, *en face* images illustrated clear delineation between gastric mucosa on the left (distal) and esophageal mucosa on the right (proximal). Several proximal regions with strikingly atypical glandular structures consistent with BE were observed. Glands were ovular or round in cross-section and were typically ~150 μm in length (range 90 – 500 μm). BE regions were surrounded by normal squamous mucosa, illustrating the potential difficulty in detecting small glandular islands with 2D-OCT or random biopsy. Cross-sectional images (Figure 1D, E) at multiple positions in the 3D-OCT volume revealed clear differences in layered architecture between gastric, normal squamous, and BE regions. A longitudinal cross-section (Figure 1D) showed normal gastric mucosa with a vertical pit pattern and reduced light penetration, consistent with previous 2D-OCT studies [14]. A ~3 mm length of normal squamous mucosa was found adjacent to a ~5 mm BE section. In cross-section (Figure 1E), BE regions exhibited distortion of the layered architecture and abnormal glandular features.
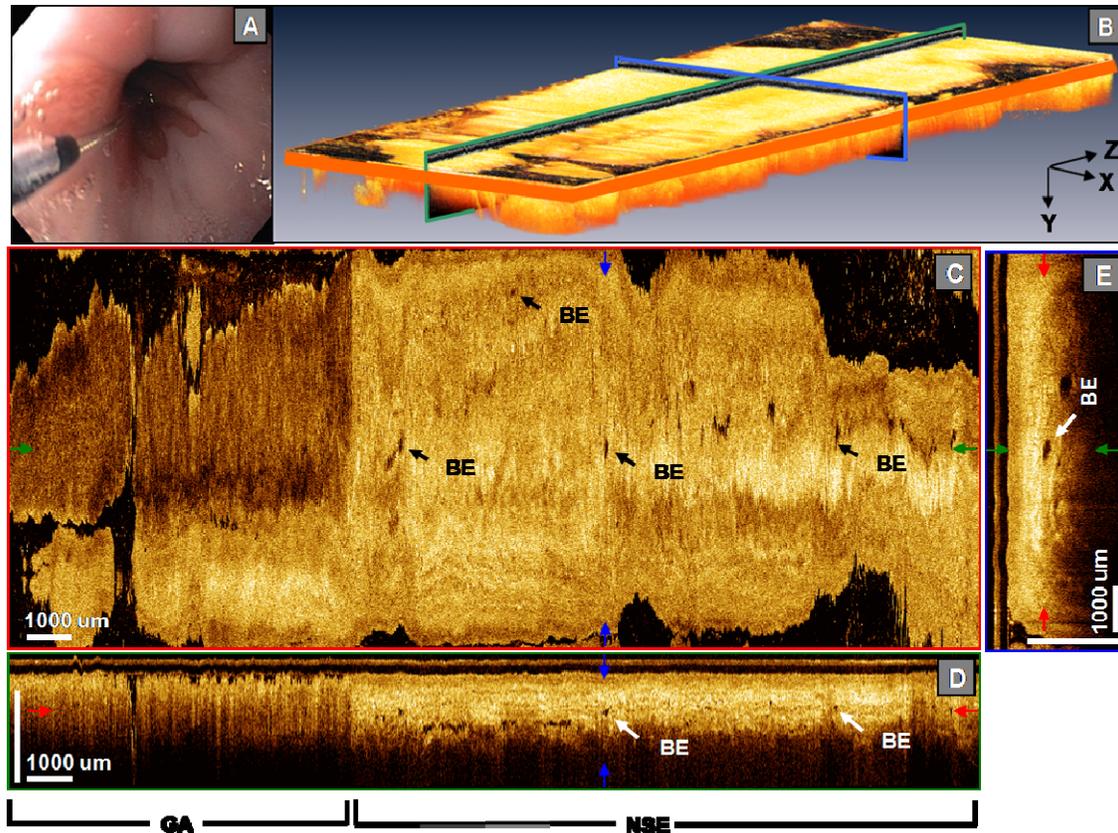
Figure 2. 3D-OCT images of a patient's distal esophagus previously treated with RFA due to BE. A: Conventional endoscopic view from the GEJ. B: Volume rendering showing location of orthogonal cut planes. C: *En face* XZ image of epithelium at 390 um tissue depth. Scattered, buried glandular features are apparent (BE) beneath NSE. D: YZ Cross-section. Gastric (GA) and NSE regions can be distinguished. Scattered buried glands (BE) are located 350 – 400 um beneath tissue surface. E: XZ cross-section. Hyperintense striations in the lamina propria and an isolated gland are visible.

Comparison to biopsy from the same area (Figure 1F) showed good correlation to 3D-OCT findings, with numerous glands and distorted layered architecture visible.

The RFA-treated BE patient, shown in figure 2, was a 72 year old male with long-segment BE near the GE junction first diagnosed in 1996. The patient was on PPI therapy for 12 years and had received three RFA treatments since March 2007, with the most recent treatment 9 months prior to 3D-OCT imaging. Conventional endoscopic examination of the distal esophagus (Figure 2A) showed a normal GE junction with no evidence of residual or buried BE. Figure 2B shows 3D-OCT volumetric rendering data spanning the GEJ. At a tissue depth of 390 μm (Figure 2C), *en face* images showed clear delineation between gastric mucosa on the left (distal) and esophageal mucosa on the right (proximal). The *en face* image appeared unremarkable aside from scattered glandular structures of a size and shape consistent with BE glands. Cross-sectional images (Figure 2D, E) revealed deeply-buried glands beneath ~350 μm (range 300 – 500 μm) of comparatively normal epithelial and lamina propria layers. The normal appearance of the epithelium on top of the glands suggests this is neosquamous epithelium which regenerated following RFA. Subtle horizontal striations were visible in the lamina propria, indicating possible fibrotic response to RFA. Biopsy specimens from this area contained gastric mucosa and GEJ tissue with no evidence of buried BE glands. This is not surprising given the scattered and sparse nature of the glands visible under 3D-OCT.

DISCUSSION

3D-OCT endomicroscopy examination provides several important benefits for assessing BE patients prior to and following ablative therapies such as RFA. 3D-OCT enables comprehensive and minimally invasive assessment of glandular microstructure over a surface area of 160 mm^2 with a tissue imaging depth of 1.6 mm. One standard pinch biopsy specimen, by comparison, typically samples a 4 mm^2 surface area with a penetration of <1 mm. The significantly increased volume which is analyzed by 3D-OCT compared to traditional pinch biopsy could reduce random sampling errors by guiding biopsy excision, leading to improved detection of buried BE glands after therapy and reduced histology processing loads. Single radial OCT frames can be continuously acquired and displayed at up to 60 frames/second, giving the endoscopist real-time information on subsurface tissue architectural morphology. A complete 3D-OCT dataset can be acquired in 20 seconds, suggesting the possibility of volumetric assessment during the endoscopy procedure as opposed to waiting days for histology processing and analysis.

With 3D-OCT endomicroscopy, *en face* tissue sections can be visualized at arbitrary axial positions to determine the depth, density, and location of untreated, residual, or buried BE glands. 3D-OCT can also visualize NSE in the regions treated with ablative procedures or, potentially, with PPI therapies to assess therapeutic efficacy. Cross-sectional image slices can be precisely aligned to *en face* features and anatomic landmarks such as the gastro-esophageal junction, which could greatly improve the ability to co-register multiple 3D-OCT datasets acquired in the same patient at different time points. This capability may prove beneficial for studying the long-term effects of BE therapies such as RFA. Co-registered cross sectional and *en face* evaluation also enables complete quantification of gland size and depth for possible use in treatment planning and follow-up assessment. The large field of view and high spatial resolution of 3D-OCT endomicroscopy allows the clinician to detect small, scattered glands that persist or recur after RFA treatment with potentially reduced sampling errors compared to conventional video endoscopy and excisional biopsy. In comparison to confocal endoscopic microscopy, 3D-OCT provides orders-of-magnitude larger fields of view with increased imaging depths at the expense of decreased transverse resolution. In the future, 3D-OCT could be used to guide biopsy for enhanced detection of buried BE glands or ultimately to make appropriate treatment decisions in real time upon discovery and analysis of BE glands.

CONCLUSIONS

While endoscopic 3D-OCT does not possess the same magnification or contrast as conventional histopathologic analysis, it is capable of visualizing large tissue volumes with greatly reduced potential for sampling error compared to excisional biopsy. The ability to detect neo-squamous mucosa, small regions of untreated BE, and buried subsurface features such as esophageal glands over a region consistent with an RFA electrode makes 3D-OCT an ideal tool for assessing response to RFA and possibly guiding re-treatments.

ACKNOWLEDGEMENT

REFERENCES

1. R.D. Odze and G.Y. Lauwers, "Histopathology of Barrett's esophagus after ablation and endoscopic mucosal resection therapy," Endoscopy **40**, 1008-1015 (2008).
2. H. Lantz, "Barrett's esophagus and argon plasma coagulation: Buried trouble?," American Journal of Gastroenterology **98**, 1647-1649 (2003).
3. D. Huang, E.A. Swanson, C.P. Lin, J.S. Schuman, W.G. Stinson, W. Chang, M.R. Hee, T. Flotte, K. Gregory, C.A. Puliafito, and J.G. Fujimoto, "Optical Coherence Tomography," Science **254**, 1178-1181 (1991).
4. G.J. Tearney, M.E. Brezinski, B.E. Bouma, S.A. Boppart, C. Pitvis, J.F. Southern, and J.G. Fujimoto, "In vivo endoscopic optical biopsy with optical coherence tomography," Science **276**, 2037-2039 (1997).
5. S.H. Yun, G.J. Tearney, B.J. Vakoc, M. Shishkov, W.Y. Oh, A.E. Desjardins, M.J. Suter, R.C. Chan, J.A. Evans, I.K. Jang, N.S. Nishioka, J.F. de Boer, and B.E. Bouma, "Comprehensive volumetric optical microscopy in vivo," Nature Medicine **12**, 1429-1433 (2006).
6. D.C. Adler, Y. Chen, R. Huber, J. Schmitt, J. Connolly, and J.G. Fujimoto, "Three-dimensional endomicroscopy using optical coherence tomography," Nature Photonics **1**, 709-716 (2007).
7. J.P. Su, J. Zhang, L.F. Yu, H.G. Colt, M. Brenner, and Z.P. Chen, "Real-time swept source optical coherence tomography imaging of the human airway using a microelectromechanical system endoscope and digital signal processor," Journal of Biomedical Optics **13(3)**, 030506 (2008).
8. D.C. Adler, C. Zhou, T.-H. Tsai, H.-C. Lee, L. Becker, J.M. Schmitt, Q. Huang, J.G. Fujimoto, and H. Mashimo, "Three-dimensional optical coherence tomography examination of non-ablated Barrett's esophagus and buried glands beneath neo-squamous epithelium following radiofrequency ablation," Endoscopy **41**, 804–807 (2009).
9. D.C. Adler, C. Zhou, T.-H. Tsai, J. Schmitt, Q. Huang, H. Mashimo, and J.G. Fujimoto, "Three-dimensional endomicroscopy of the human colon using optical coherence tomography," Optics Express **17**, 784-796 (2009).
10. M.J. Suter, B.J. Vakoc, P.S. Yachimski, M. Shishkov, G.Y. Lauwers, M. Mino-Kenudson, B.E. Bouma, N.S. Nishioka, and G.J. Tearney, "Comprehensive microscopy of the esophagus in human patients with optical frequency domain imaging," Gastrointestinal Endoscopy **68**, 745-753 (2008).
11. X.D. Li, S.A. Boppart, J. Van Dam, H. Mashimo, M. Mutinga, W. Drexler, M. Klein, C. Pitris, M.L. Krinsky, M.E. Brezinski, and J.G. Fujimoto, "Optical coherence tomography: advanced technology for the endoscopic imaging of Barrett's esophagus," Endoscopy **32**, 921-30 (2000).
12. J.M. Poneros, S. Brand, B.E. Bouma, G.J. Tearney, C.C. Compton, and N.S. Nishioka, "Diagnosis of specialized intestinal metaplasia by optical coherence tomography," Gastroenterology **120**, 7-12 (2001).
13. G. Isenberg, M.V. Sivak, A. Chak, R.C.K. Wong, J.E. Willis, B. Wolf, D.Y. Rowland, A. Das, and A. Rollins, "Accuracy of endoscopic optical coherence tomography in the detection of dysplasia in Barrett's esophagus: a prospective, double-blinded study," Gastrointestinal Endoscopy **62**, 825-831 (2005).
14. Y. Chen, A.D. Aguirre, P.L. Hsiung, S. Desai, P.R. Herz, M. Pedrosa, Q. Huang, M. Figueiredo, S.W. Huang, A. Koski, J.M. Schmitt, J.G. Fujimoto, and H. Mashimo, "Ultrahigh resolution optical coherence tomography of Barrett's esophagus: preliminary descriptive clinical study correlating images with histology," Endoscopy **39**, 599-605 (2007).